

*Optimization of Air-Sparged Plutonium  
Oxalate/Hydroxide Precipitators*

**Los Alamos**  
NATIONAL LABORATORY

*Los Alamos National Laboratory is operated by the University of California  
for the United States Department of Energy under contract W-7405-ENG-36.*

*An Affirmative Action/Equal Opportunity Employer*

*This report was prepared as an account of work sponsored by an agency of the United States Government. Neither The Regents of the University of California, the United States Government nor any agency thereof, nor any of their employees, makes any warranty, express or implied, or assumes any legal liability or responsibility for the accuracy, completeness, or usefulness of any information, apparatus, product, or process disclosed, or represents that its use would not infringe privately owned rights. Reference herein to any specific commercial product, process, or service by trade name, trademark, manufacturer, or otherwise, does not necessarily constitute or imply its endorsement, recommendation, or favoring by The Regents of the University of California, the United States Government, or any agency thereof. The views and opinions of authors expressed herein do not necessarily state or reflect those of The Regents of the University of California, the United States Government, or any agency thereof. Los Alamos National Laboratory strongly supports academic freedom and a researcher's right to publish; as an institution, however, the Laboratory does not endorse the viewpoints of a publication or guarantee its technical correctness.*

*Optimization of Air-Sparged Plutonium  
Oxalate/Hydroxide Precipitators*

*W. Brian VanderHeyden\**

*S. L. Yarbrow\*\**

*K. W. Fife\*\**

*\*Fluid Dynamics Group, Theoretical Division, Los Alamos National Laboratory*

*\*\*Actinide Process Chemistry Group, Nuclear Materials Technology Division, Los Alamos National Laboratory*

# **Optimization of Air-Sparged Plutonium Oxalate/Hydroxide Precipitators**

by

**W. Brian VanderHeyden, S. L. Yarbrow, and K. W. Fife**

## **ABSTRACT**

The high cost of waste management and experimental work makes numerical modeling an inexpensive and attractive tool for optimizing and understanding complex chemical processes. Multiphase "bubble" columns are used extensively at the Los Alamos Plutonium Facility for a variety of different applications. No moving parts and efficient mixing characteristics allow them to be used in glovebox operations. Initially, a bubble column for oxalate precipitations is being modeled to identify the effect of various design parameters such as, draft tube location, air sparge rate and vessel geometry. Two-dimensional planar and axisymmetric models have been completed and successfully compared to literature data. Also, a preliminary three-dimensional model has been completed. These results are discussed in this report along with future work.

## **INTRODUCTION**

### **Objective**

Successful completion of the Defense Nuclear Facilities Safety Board (DNFSB) 94-1 program is a high priority for the Los Alamos National Laboratory. Many of the residues scheduled for recovery are currently liquids, such as analytical returns, or are solids that will be leached or dissolved to remove the plutonium. Therefore, all of the plutonium will have to be precipitated at some point to concentrate the plutonium as an oxide that is suitable for the long-term repackaging program.

The Fluid Dynamics Group's (T-3's) multiphase flow code library, CFDLIB, has been used to simulate multiphase flows in two and three dimensions with complex geometries in a variety of industrial and defense related problems. A project has also been started using CFDLIB to analyze the flow and process chemistry in the plutonium precipitators with an aim toward providing insight into the effects of vessel geometries and the bubble and particle scale dynamics which govern the efficiencies of the precipitators. CFDLIB also might be able to simulate proposed modes of operation of the precipitators to provide updated guidelines for operations.

This research project will also include an experimental component in which data will be collected from precipitators to help validate and guide the multiphase exchange and turbulence closure models that will have to be incorporated in CFDLIB to simulate the precipitators. The initial experiments and data should be taken once a preliminary simulation capability is demonstrated. The simulation results will help target the experimental work so that it is most useful for developing the closure models. The FY 1997 Technical Task Plan for this project is provided as the Appendix to this report.

## Benefits

Current waste acceptance criteria are being negotiated that will drive the plutonium discard limit to less than or equal to 0.5 microcurie per liter for liquid waste. Optimizing the recovery of plutonium from the precipitation units will help meet or exceed this limit and reduce the cost of downstream waste processing operations. Current precipitation filtrates are 9400 microcuries per liter. The solubility limit for Pu(III) oxalates, shown in Figure 1, is approximately 960 microcuries per liter (Yarbro, 1991).

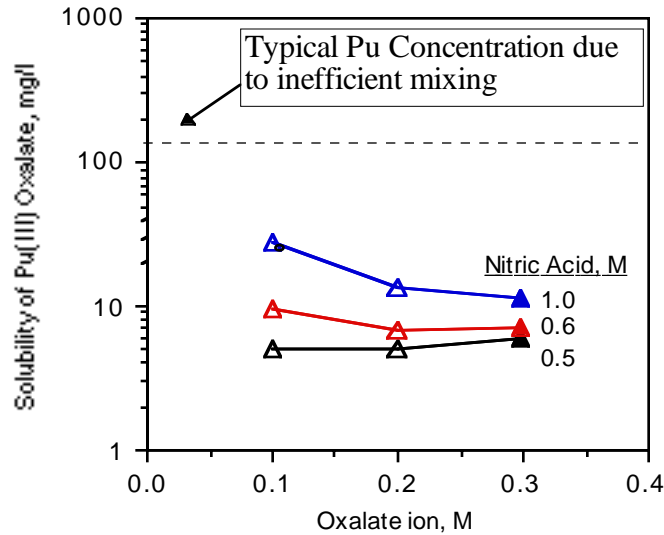


**Figure 1. Equilibrium and actual Pu(III) concentrations at various oxalate and nitric acid concentrations.**

Waste management costs are high for radioactive wastes and there is a large difference between the costs of low-level and transuranic wastes. A comparison of waste management costs is shown below in Table 1. Transuranic (TRU) waste can cost up to \$12,000 per 55 gallon drum to process and dispose, in contrast to low-level waste (LLW), which only costs about \$1000 per drum. Therefore, significant cost savings will be achieved by having higher plutonium recovery efficiencies. Also, the precipitation conditions affect the filtration characteristics of the final product. Better cakes mean faster filtration times and lower overall exposures to the operators.

**Table 1. Comparison of FY94 Average Waste Management Costs for Various Waste Types (Matysiak, 1994)**

Waste Type	Direct Costs	Indirect Costs	Total Costs
Low-Level - m <sup>3</sup>	\$2596	\$2838	\$5434
Transuranic - m <sup>3</sup>	\$11160	\$15852	\$27012

## CFDLIB

Reactive multiphase flows are found in many of the processes across the spectrum of manufacturing and processing industries. One example is the widespread use of circulating fluidized beds used in oil refining to catalytically crack heavy oil into gasoline. Another is gas-sparged draft-tube precipitators used for the recovery of plutonium at Technical Area 55 (TA-55). In many cases, control of the spatial distribution of the individual phases of the multiphase flow can have a large impact on the efficiency of these processes. With the recent advances in the size and speed of modern supercomputers and with the continuing improvement in the state of the art of the mathematical description of multiphase flows, it is becoming possible to use computer simulation to scale up, optimize and design multiphase flow equipment more accurately and precisely than is possible with traditional methods.

Due to the complexity of multiphase flows and also to the intensive nature of the computer calculations used to solve their governing equations, however, ongoing research is needed to improve both the mathematical description and the numerical solution of the multiphase flow equations. Toward this end, our research has focused on developing a multipurpose computer simulation code library, called CFDLIB (Computational Fluid Dynamics Library), which has the capability of simulating industrially relevant reactive multiphase flows in geometrically complicated vessels. CFDLIB serves as a vehicle for testing new ideas on modeling and computing reactive multiphase flows. The following provides a brief technical description of CFDLIB and a short summary of current technical applications.

### Technical Description

CFDLIB is a library of flow simulation codes which all share a common data structure. The codes in the library simulate the effects of turbulence, interphase mass, momentum and heat exchange, chemical reactions, and evaporation and condensation in essentially an arbitrary number of phases with an arbitrary number of chemical species in both two and three dimensions. CFDLIB is designed to run on UNIX workstations, clusters of work stations, Cray vector supercomputers and parallel supercomputers.

CFDLIB uses state-of-the-art numerical techniques to achieve high accuracy and computational speed. All library codes are based on the finite-volume discretization technique. All data are located at the center of the individual cells that make up a given flow domain. Currently, a multiblock data structure is employed to enable the treatment of complex geometries with a high degree of computational efficiency. A new unstructured grid version of CFDLIB is under development which will further enhance the user's ability to compute geometrically complex flows. CFDLIB employs second-order total variation diminishing (TVD) advection to minimize artificial numerical diffusion. Van-Leer gradient limiting ensures that no artificial extrema are introduced by the numerical method.

Governing Equations. The motion of each phase is governed by mass, momentum and energy conservation equations (Kashiwa and Rauenzahn, 1994). The mass conservation equation for each phase is given, assuming no interphase mass exchange, by

$$\frac{\partial \rho_k}{\partial t} + \nabla \cdot \rho_k \mathbf{u}_k = 0 \quad (1)$$

where the subscript k denotes the kth phase in the flow, t is time,  $\nabla$  is the divergence operator,  $\rho_k$  is the mass of phase k per unit volume, and  $\mathbf{u}_k$  is the mean local velocity of

phase k. The first term in equation (1) is the time rate of change of phase k mass at a point. The second term is the net inflow of phase k mass at a point.

The momentum conservation equation for phase k is given, assuming no mass exchange, by

$$\rho_k \frac{d\mathbf{u}_k}{dt} = -\theta_k \nabla p + \sum_l \mathbf{F}_{lk} - \nabla \cdot \rho_k \mathbf{R}_k + \rho_k \mathbf{g} \quad (2)$$

where  $\theta_k$  is the volume fraction of phase k, p is the common pressure,  $\mathbf{F}_{lk}$  is the momentum exchange force due to the action of phase l on phase k,  $\mathbf{R}_k$  is the turbulent Reynolds stress tensor for phase k and  $\mathbf{g}$  is the acceleration due to gravity. The term on the left-hand side of equation (2) is the time rate of change of phase k momentum at a point. The terms on the right-hand side of equation (2) are the pressure gradient forces, the momentum exchange forces, the turbulence forces and the body forces acting on phase k at a point, respectively.

Both the momentum exchange force and the Reynolds stress are quantities for which models must be introduced and therefore introduce the greatest amount of uncertainty into multiphase flow simulations. These terms are the subject of ongoing research. Nevertheless, approximate models may be introduced and used with a reasonable level of confidence as long as one is careful to validate solutions of the equations against suitable experimental data. In the following, candidate models are introduced and tested against data from experimental applications similar to the TA-55 precipitators.

Closure Models. The momentum exchange force arises from the familiar effects of drag and less familiar phenomena such as added- or apparent-mass wherein the inertia of one phase is felt by another. A model for  $\mathbf{F}_{lk}$  which accounts for these two exchange effects for a fluid/particle system is given by

$$\mathbf{F}_{lk} = \theta_l \theta_k K_{lk} (\mathbf{u}_l - \mathbf{u}_k) + \theta_l \theta_k \rho_{fluid} C_a \left( \frac{d\mathbf{u}_l}{dt} - \frac{d\mathbf{u}_k}{dt} \right) \quad (3)$$

$$K_{lk} = \frac{3}{4} \rho_{fluid} C_d \frac{|\mathbf{u}_l - \mathbf{u}_k|}{d_p} \frac{1}{\theta_{fluid}^{2.65}} \quad (4)$$

The first term in equation (3) accounts for steady-state drag and the second term accounts for the added-mass effect. In these equations,  $C_a$  is a dimensionless constant and is typically taken equal to 0.5, a value appropriate for a single sphere immersed in a large expanse of ideal nonviscous fluid.  $C_d$  is the drag coefficient and  $d_p$  is the spherical particle diameter. The last factor in equation (4) accounts for the increased drag that occurs as the fluid volume fraction decreases from unity. Equations (3) and (4) will be used as our base momentum exchange model in these studies.

The effect of additional momentum exchange due to turbulent dispersion was also considered in these studies. Simonin and Viollet (1989) argue that fluid turbulence produces an additional exchange force of the form

$$(\mathbf{F}_{lk})_{dispersion} = -\theta_l \theta_k K_{lk} \nu_p \nabla \theta_k \quad (5)$$

where  $v_p$  is a particle or bubble turbulent diffusion coefficient. This momentum exchange term will tend to disperse or smooth out gradients in volume fractions.

The turbulent Reynolds stress term,  $\mathbf{R}_k$ , in equation (2) accounts for diffusion of momentum due to fluctuation motion. This is the least well understood term in the momentum conservation equation and will therefore introduce the greatest degree of uncertainty. The simplest model for the Reynolds stress is given by assuming that the effect can be characterized by a so-called Boussinesq form with an eddy diffusivity:

$$\mathbf{R}_k = -v_t \left( \nabla \mathbf{u}_k + (\nabla \mathbf{u}_k)^t \right) + \frac{2}{3} k_k \mathbf{I} \quad (6)$$

where  $v_t$  is the turbulent eddy diffusivity,  $k_k$  is the turbulent kinetic energy and  $\mathbf{I}$  is the identity tensor. The eddy diffusivity is most simply estimated using the mixing length model

$$v_t = \mathcal{L}^2 |\nabla \mathbf{u}_k| \quad (7)$$

where  $\mathcal{L}$  is the so-called mixing length. In this work, the mixing length was taken to be of the order of the computational cell size in order to capture subgrid-scale turbulent momentum transfer. Also, for cases in which the mixing length model was used, the second term in equation (6) was neglected due to lack of a good simple model.

More sophisticated turbulence models relate the eddy diffusivity as a function of the turbulent kinetic energy and the turbulence energy dissipation rate,  $\varepsilon_k$ :

$$v_t = c_\mu \frac{k_k^2}{\varepsilon_k} \quad (8)$$

where the  $k_k$  and  $\varepsilon_k$  are obtained from conservation equations taken directly from single phase high Reynolds number theory. The dimensionless constant,  $c_\mu$ , is taken to be equal to 0.09 from single phase theory. In our work to date, we have examined the effects of both the simple Prandtl mixing length model and a more sophisticated multiphase “k-epsilon” turbulence model. For the more sophisticated case, the second term in equation (6) was retained since  $k_k$ , turbulence energy, was explicitly calculated. This term, when inserted into the momentum conservation equation can provide spreading effects similar to the exchange model of Simonin and Viollet (1989).

In addition to the mass and momentum equations, a conservation equation for internal energy may be solved if one is interested in variations in the temperature of the flow. Also, an arbitrary number of scalars and chemical species can be transported with each phase. Examples of transported scalars include turbulent kinetic energy and bubble size.

## **Applications**

The applications addressed using CFDLIB include examples from several industries. Two examples of multiphase flow from the petroleum industry include the simulation of gas-liquid separation in a residual oil catalytic hydrocracker and the simulation of oil vaporization and catalyst motion in the injection zone of a fluid catalytic cracking unit. CFDLIB is being used to study the motion of dense sand-resin mixtures used to make sand-cast molds for the manufacture of automobile engine blocks. Other applications include the simulation of a 4-phase iron smelter. CFDLIB has also been used in a number of defense applications.

## DRAFT-TUBE BUBBLE COLUMN SIMULATIONS

Our initial efforts toward the development of a comprehensive simulation tool for the TA-55 plutonium precipitators have focused on benchmarking the CFDLIB code against two experimental data sets from the open literature (Freedman and Davidson, 1969 and Pironti et al., 1995) and an initial 3-D demonstration simulation of the multiphase flow in the Rocky Flats precipitator. In what follows, we provide a progress report on these studies.

### Freedman and Davidson Draft-Tube Bubble Column

Freedman and Davidson (1969) studied the effect of gas rate, column height and draft-tube diameter on gas holdup in the draft tube and annular space or annulus of a draft-tube bubble column. Their experimental apparatus consisted of a 9-inch diameter column with 4-, 6- and 8-inch diameter perspex and sheet metal draft tubes with lengths of 100, 150 and 200 cm. The draft tubes were supported 6 cm above the base of the column and an overflow pipe maintained a free surface 6 cm above the top of the draft tube. The apparatus is depicted schematically in Figure 2. The liquid phase was water and the column was

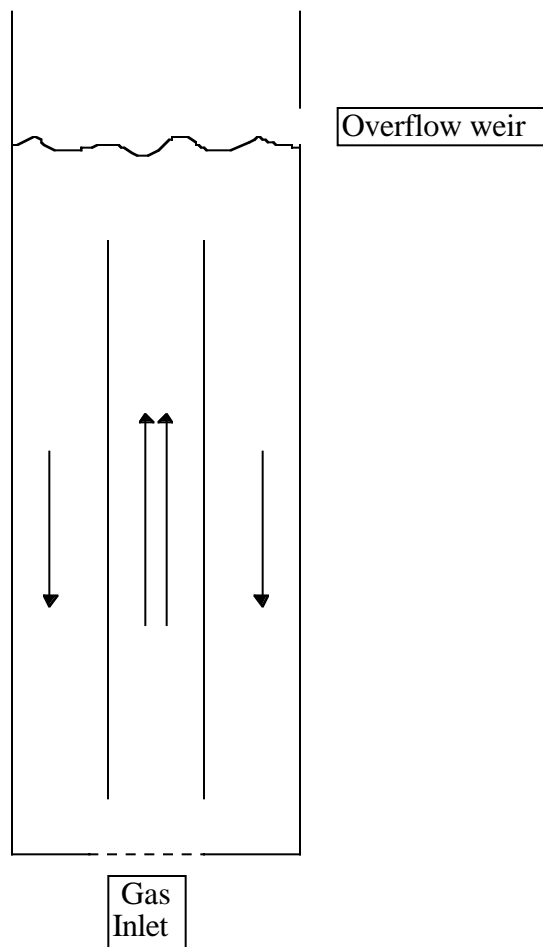


**Figure 2. Schematic diagram of Freedman and Davidson draft-tube bubble column.**

operated with no net liquid flow. Gas was sparged into the column through perforated plates positioned directly below the draft tubes. Most bubbles were observed to be in the 3-8 mm diameter range. A “small proportion” of the bubbles had diameters closer to 1 mm (Freedman and Davidson, 1969). The gas volume fractions in the draft tube and in the annulus were determined from pressure drop measurements. The gas volume fraction in the draft tube was also independently determined from conductance measurements. Gas superficial velocities ranging from 2 to 12 cm/sec based on the draft-tube cross-sectional area were used. Minimal bubble coalescence was observed.

**Simulations.** The Freedman and Davidson draft-tube experiments were modeled using the 2-D incompressible code, MFMAC (Multi-Fluid Marker and Cell), from CFDLIB on a Silicon Graphics Inc. (SGI) workstation with a 194 MHz R10000 microprocessor and a R100010 floating point coprocessor. Attention was focused on the intermediate case with a tube-height of 156 cm and a diameter of 6 inches. Runs were made for the three superficial gas velocities investigated by Freedman and Davidson of 2, 6 and 10 cm/sec. The effects of momentum exchange models and turbulence models were examined.

Figure 3 shows the computational mesh used in the cases. Axisymmetry was assumed for all computations. Near the ends of the draft tube, the vertical cell dimension was taken as 1 cm. Away from the ends of the tube, the vertical cell dimension was allowed to grow in a smooth fashion as shown to help reduce the computational burden in regions where the

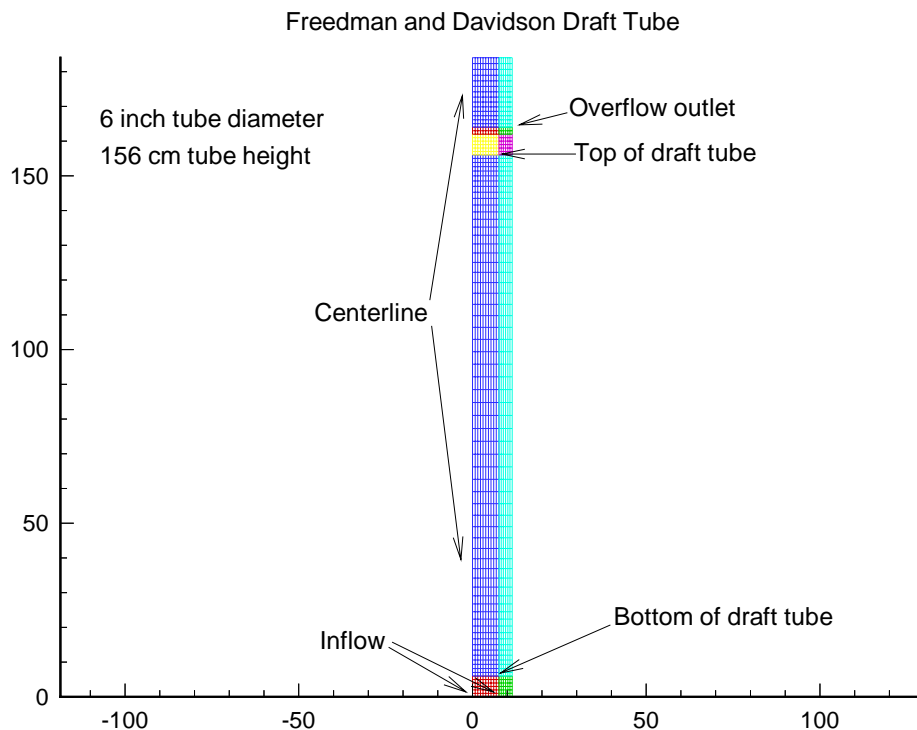


**Figure 3.** Computational mesh for the Freedman and Davidson draft-tube bubble column simulations. The left boundary is the center line axis of symmetry. The different blocks used to construct the mesh are indicated by the shading. Vertical and horizontal axis units are centimeters.

flow was expected to be essentially one-dimensional. The maximum vertical cell dimension was 3.73 cm. The horizontal cell dimension was 0.76 cm for the region in the draft tube and 0.64 cm in the annular section.

Boundary conditions were imposed on the phase velocities, volume fractions and the pressure. On solid walls, a “law-of-the-wall” boundary condition was used for the tangential component of liquid velocity; a free-slip condition was used for the gas tangential velocity. The normal components of the liquid and gas velocity were set to zero on solid walls. At the inlet, uniform inflow velocities were imposed for the gas. The inflow volume fraction of gas was set to 100%. Zero normal derivative conditions were used along the outflow boundary on all fields. For these calculations, it was assumed that the flow was axisymmetric so symmetry conditions were imposed along the center line.

Three sets of calculations were performed to investigate the effects of the different exchange and turbulence models described previously. Table 2 provides a description of these cases. For all cases, the drag coefficient was specified to give a bubble rise velocity of 23.5 cm/sec. This value is appropriate for air-water systems (Freedman and Davidson, 1969). The added-mass coefficient was taken as 0.5. The Prandtl mixing length was chosen as 0.5 cm to account for the subgrid scale turbulent momentum diffusion.

The initial conditions for the calculations were as follows. The column was filled to the overflow level with motionless liquid. Above the overflow level was motionless gas. The gas inflow rate was then ramped to its steady-state value over the first 20 seconds of real time for each experimental case. This was done to prevent a surge of high gas volume from an abrupt start-up which pushed too much of the initial charge of liquid out of the column. Simulations were continued to 30 seconds, real time, by which time a statistical steady state was achieved. The results were time averaged from 20 to 30 seconds. The Prandtl mixing length calculations took approximately an hour of central processing unit (CPU) time. The multiphase k-epsilon calculations took a little over 3.5 CPU hours due to smaller time step limitations introduced by stronger turbulent viscosity.

**Results.** The results of the calculations are shown in Figures 4 through 6 as contour plots of gas volume fraction overlaid by liquid velocity vectors. Figure 4 shows the results from the base-case calculations using the Prandtl mixing length model for turbulent momentum diffusion and the base momentum exchange models for the superficial gas velocity,  $U_d$ , of 2, 6 and 10 cm/sec, respectively. Figure 5 shows the corresponding results from the calculations after adding the Simonin and Viollet (1989) momentum exchange model and Figure 6 shows the corresponding results from the calculations using a multiphase k-epsilon turbulence model.

In each case, the average gas volume fraction in the draft tube and in the annulus of the column was determined from the simulation data. These results are plotted against the experimental data in Figures 7a, b, and c as a function of the draft-tube gas superficial velocity.

**Table 2. Modeling Cases for the Freedman and Davidson Draft-Tube Simulations**

Case Name	Momentum Exchange Model	Turbulence Model
Base	equations (3) and (4)	Prandtl mixing length
Simonin exchange model	equations (3), (4) plus (5)	Prandtl mixing length
Multiphase “k-epsilon”	equations (3) and (4)	multiphase k-epsilon

Freedman and Davidson Draft Tube Bubble Column - Base Case  
Tube Diameter = 6 inches, Tube Length = 156 cm

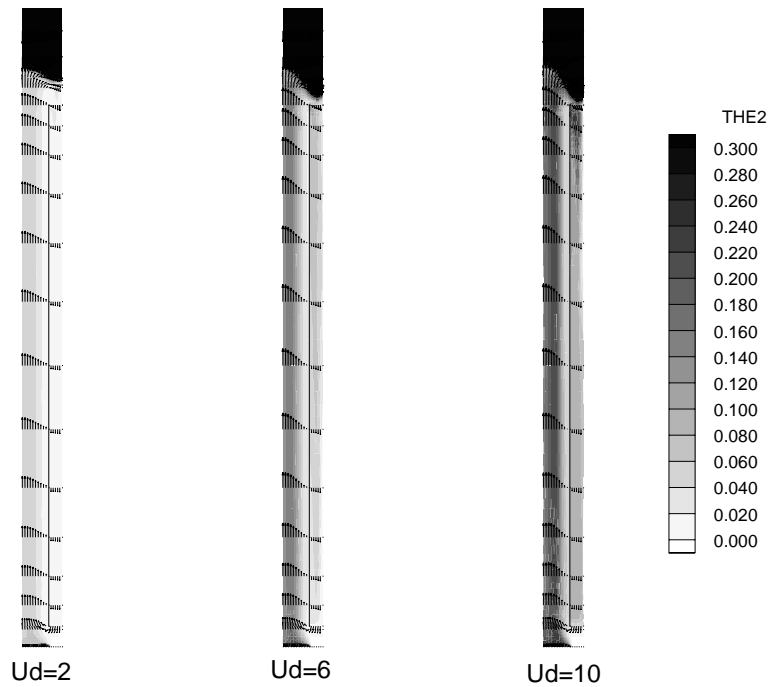


**Figure 4.** Gas volume fraction and liquid velocity for the Freedman and Davidson draft-tube bubble column simulations using a Prandtl mixing length model for turbulent momentum diffusion. The shading indicates gas volume fraction. The vectors indicate liquid velocity. The left boundary in each plot is the center line and is an axis of symmetry. Dark regions are >30% gas by volume.

Freedman and Davidson Draft Tube Bubble Column - Simonin Exchange Case  
Tube Diameter = 6 inches, Tube Length = 156 cm

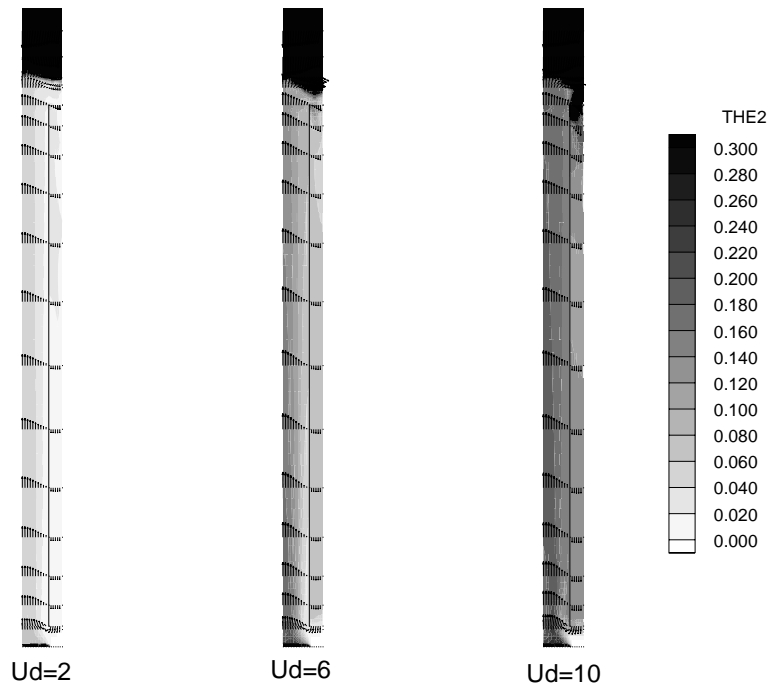


**Figure 5. Gas volume fraction and liquid velocity for the Freedman and Davidson draft-tube bubble column simulations using a Prandtl mixing length model for turbulent momentum diffusion and a Simonin and Violet exchange model.**

Freedman and Davidson Draft Tube Bubble Column - Multiphase "k-epsilon" Case  
Tube Diameter = 6 inches, Tube Length = 156 cm

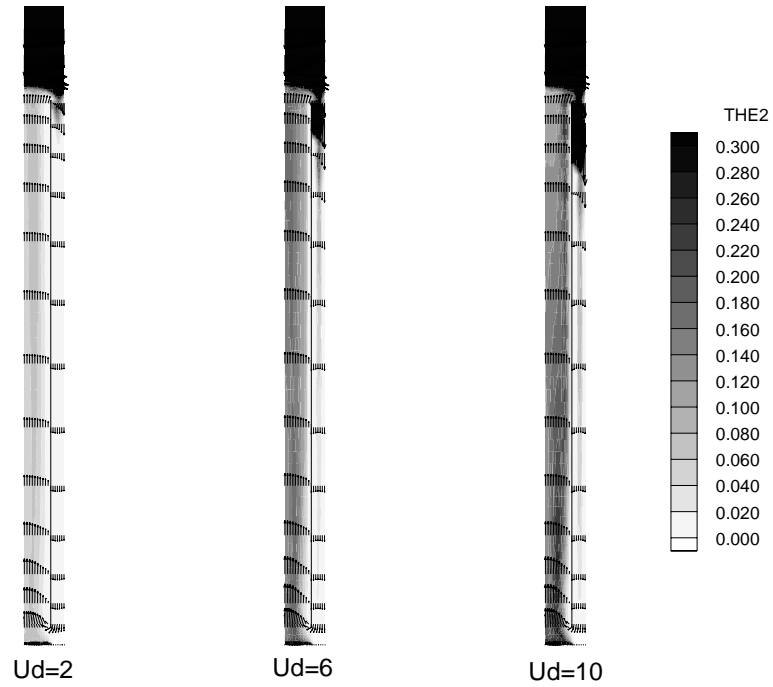


**Figure 6. Gas volume fraction and liquid velocity for the Freedman and Davidson draft-tube bubble column simulations using a multiphase “k-epsilon” turbulence model.**

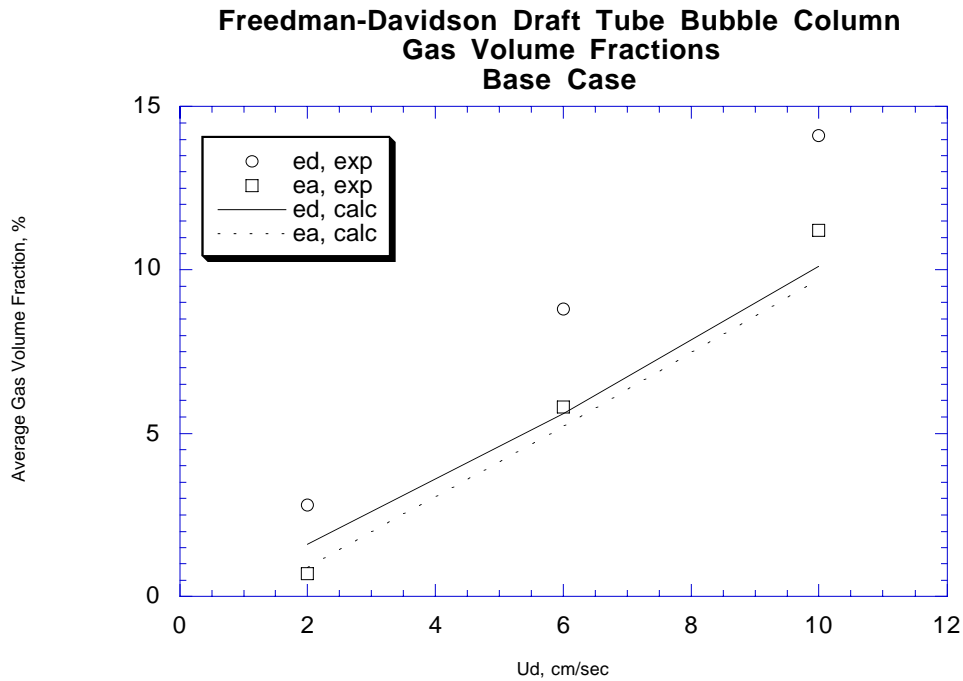


**Figure 7a.** Average gas volume fractions for the base case. In the key, ed, exp is experimental average draft tube gas volume fraction; ea, exp is experimental average annulus gas volume fraction; ed, calc is calculated average draft-tube gas volume fraction; and ea, calc is calculated average annulus gas volume fraction.

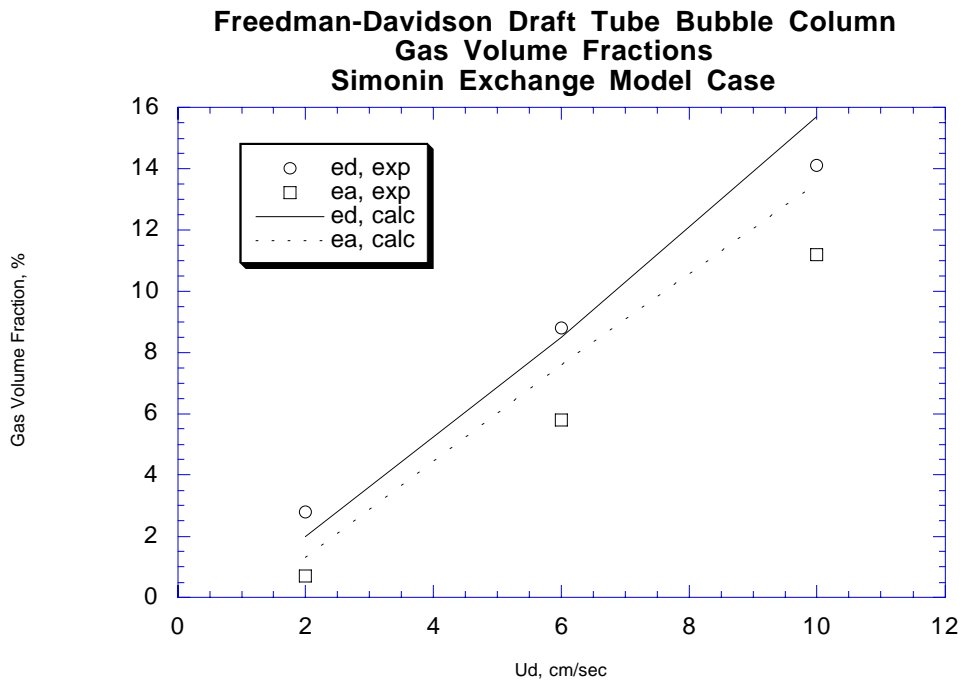


**Figure 7b.** Average gas volume fractions for the Simonin exchange model case.

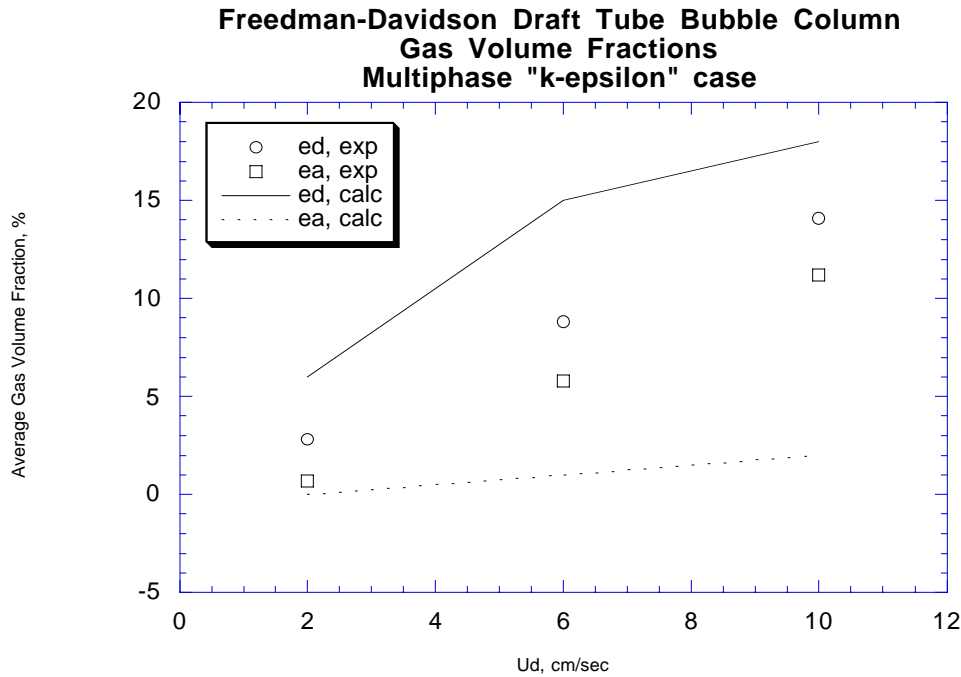


**Figure 7c. Average gas volume fractions for the multiphase “k-epsilon” turbulence model case.**

Discussion. There are a number of features worth pointing out. In the base case, the average gas volume fractions are predicted to be lower than the experimental data as can be seen in Figure 7a. Also, the predicted difference between the gas volume fraction in the tube and annulus is much smaller than the measured values. In Figure 7b, one can see that the absolute value of the gas volume fraction in the draft tube is higher and in better agreement with the experimental data for the computation using the exchange model of Simonin and Viollet (1989). The Simonin and Viollet exchange model case, however, seems to miss the prediction of the difference between the gas volume fraction in the tube and the annulus. Finally, the multiphase k-epsilon model, as seen in Figure 7c, seems to predict a large difference between the tube and annulus gas volume fractions. In fact, the difference is overpredicted.

These observations may be partially explained by the amount of spreading of the gas plume in the draft tube in each of the simulations. As can be seen by comparing Figure 4 with Figures 5 and 6, the gas in the draft tube in the base-case calculation tends to concentrate in the center leaving a relatively bubble-free liquid layer along the outer edge of the tube. This distribution of gas tends to drive liquid circulation in the tube which, in turn, lowers the over gas volume fraction in the tube. This reflects the lack of a turbulent spreading term in the base-case models.

This problem was partially remedied by using either the Simonin and Viollet exchange model or by using a multiphase k-epsilon turbulence model. As can be seen in Figures 5 and 6, these models produced more spreading of the gas plume. More study is required to understand what combinations of these models provide a more correct description of the true dynamics of these bubbly flows.

### Pironti et al. 3-Phase Draft-Tube Bubble Column

Pironti et al. (1995) studied the effect of draft-tube position in a conical-bottom cylindrical column on circulation stability and on velocity and column gas volume fraction. The most striking finding of their study was that the stability of the circulation is disrupted if the bottom of the draft tube is positioned too high above the bottom of the column.

The apparatus used by Pironti et al. consisted of a cylindrical top section with a 30 cm internal diameter and a length of 3 m. The “phase distribution” section of the apparatus attached to the bottom of the column was conical with an apex angle of 34 degrees and a length of 43 cm. The draft tube was 14 cm in internal diameter and had a length of 2 m. The wall of the draft tube was 0.5 cm thick. The draft tube was used in three different axial positions, 20, 31 and 43 cm above the tip of the conical section, respectively. Positions 2 and 3 are shown in Figure 8.

Air was introduced into the bottom of the conical section with a nozzle. All experiments were performed at room conditions. Air was the gas phase and tap water was the liquid phase. The solid phase was siliceous sand with a density of  $2.8 \text{ g/cm}^3$  and a mean diameter of 130 microns.

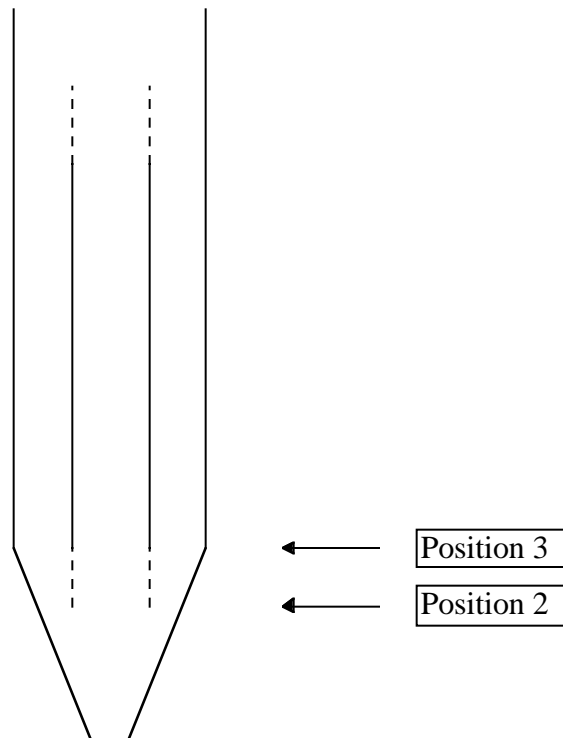


**Figure 8. Schematic diagram of the Pironti et al. conical-bottom draft-tube bubble column. Experiments were performed with the draft tube in three different vertical positions. The lowest position, Position 1, is not shown and was not considered in our studies.**

Gas volume fraction was determined from pressure differential measurements on both the annulus and the draft tube. Solids volume fraction distribution was shown to be essentially uniform by extracting samples from various flow locations.

Simulations. Figure 9 shows the mesh used for the simulation runs. A 2-dimensional planar geometry was used since 2-dimensional axisymmetric calculations encountered convergence difficulties. These difficulties were believed to be due to the substantially asymmetric nature of the actual instantaneous flow.

In the first attempt at modeling this system, the base exchange models were used. The gas-liquid drag model was the same as was used in the Freedman and Davidson draft-tube simulations. The momentum exchange coefficient between the gas and the solid material was taken as equal to the exchange coefficient between the solid and liquid. This assumption was necessary to avoid unrealistic accumulation of solids at the bottom near the jet. The physical motivation for this assumption was that the solids would likely be swept up in the wake of the bubbles and would therefore follow the gas bubbles near the jet region with a coupling similar to the liquid-solid coupling. The Prandtl mixing length model for momentum diffusion was used in these calculations with a mixing length of 0.5 cm.

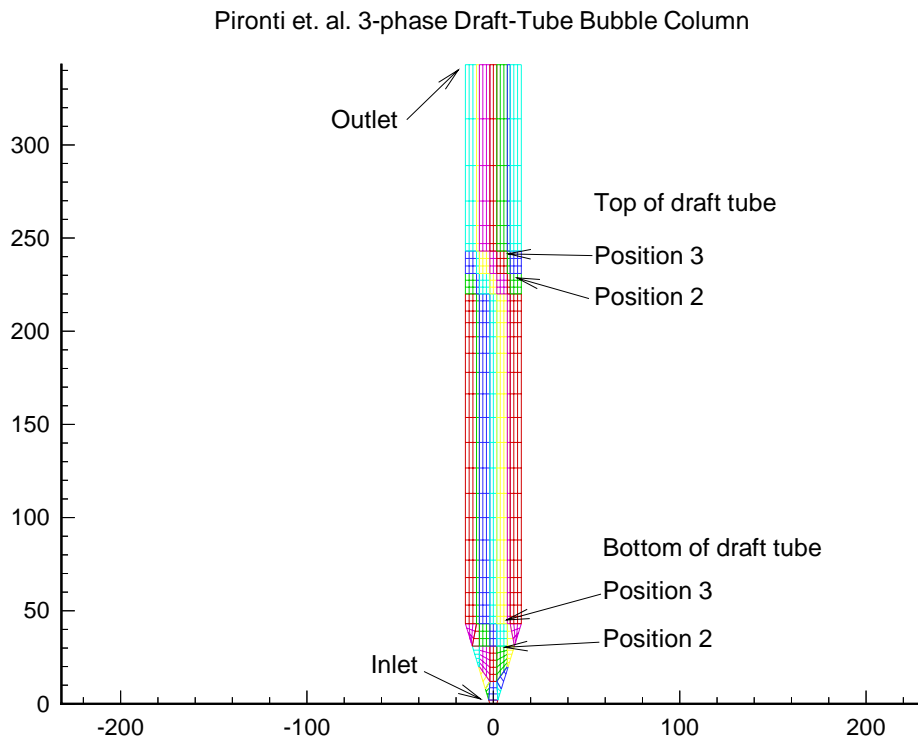


**Figure 9.** The Pironti et al. 3-phase conical-bottom draft-tube bubble column. The shading indicates the different blocks used to construct the mesh. Vertical and horizontal axis units are centimeters.

Each simulation was run for 30 seconds real time. The solutions were time averaged from 20 to 30 seconds. Each of these runs took approximately 7 hours on the SGI workstation. The base-case time-averaged results are shown in Figure 10 as gas volume fraction contours with overlaid liquid velocity vectors. These results show a qualitative difference between the two draft-tube positions similar to that reported by Pironti et al. With the draft tube in position 2, the circulation pattern is well developed with upflow in the draft tube and downflow in the annulus. With the draft tube in position 3, however, circulation is not well developed with upflow in the right annular channel. This effect is presumably due to higher placement of the draft tube which allows gas to more easily bypass the draft tube. This observation corresponds, qualitatively, to what was observed experimentally. While these qualitative results are somewhat encouraging, it must be pointed out that the simulated gas volume fractions in the columns in these cases are well above the experimentally observed values (40+% versus 20%). This inconsistency is most likely due to the fact that a significant amount of bubble coalescence occurs in the real system which is not accounted for in our base exchange model.

Pironti, et. al. 3-phase Draft-Tube Bubble Column

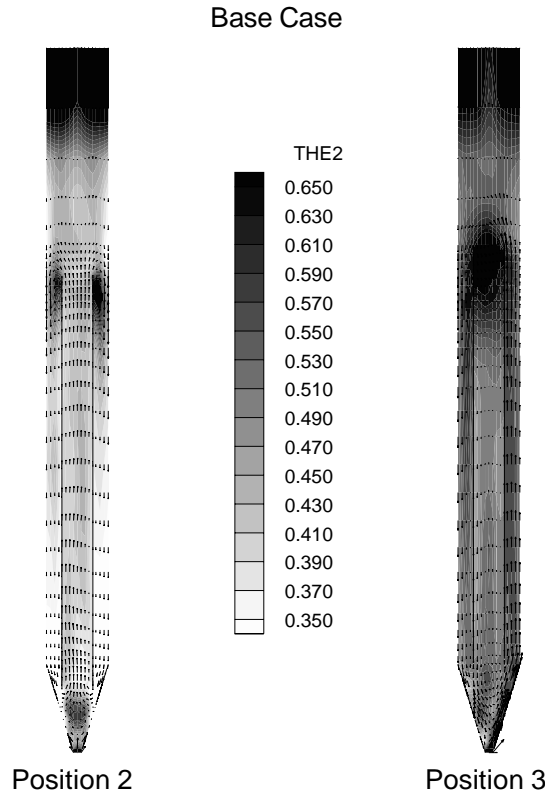


**Figure 10.** Base-case simulation of conical-bottom draft-tube bubble column with draft tube in positions 2 and 3. Shading indicates volume fraction of gas. Vectors indicate liquid velocity.

In order to try to capture the effect of bubble coalescence, a second set of calculations was performed with a simple, somewhat crude, modification to our base momentum exchange model to account for coalescence. If the local gas volume fraction reached 25%, the drag coefficient was lowered to 10% of its base value to try to mimic the effect of bubble coalescence. The results of the calculations are shown in Figure 11. As can be seen, the crude coalescence model lowered the average gas volume fraction in the column as expected. Unfortunately, this also has the effect of eliminating the differences between the two draft-tube positions. More work is required to properly capture these effects. Part of the problem with our simulations may be that a 3-dimensional treatment is required. The 2-dimensional planar geometry used in these calculations was hampered by the fact that it is impossible to preserve both the ratio of the tube and column diameters and the tube and column cross-sectional areas. Only a 2-dimensional axisymmetric or 3-dimensional treatment can do this.

Finally, it was also observed that the dispersal of the solids phase in each of our simulations was high. That is, the volume concentration of solids in the calculations was fairly uniform indicating little net settling. This was also observed experimentally. This agreement with experiment indicates that our choice of gas-solid momentum exchange model was adequate.

Pironti, et. al. 3-phase Draft-Tube Bubble Column  
Coalescence Exchange Model Case

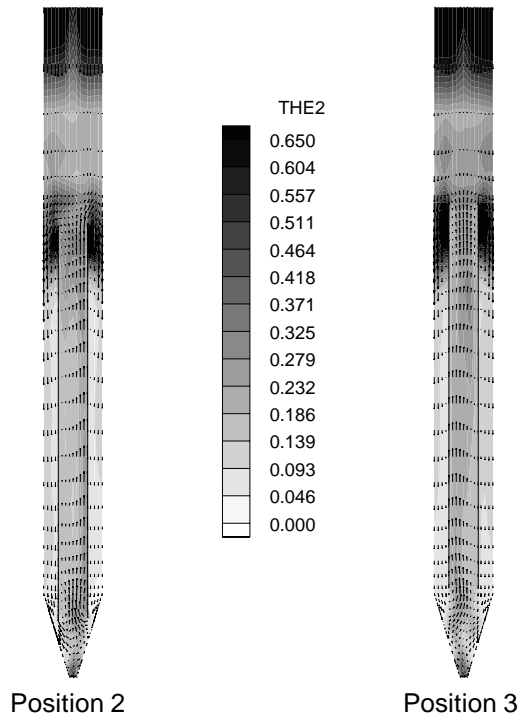


**Figure 11. Simulation of Pironti et al. conical-bottom draft-tube bubble column with the coalescence momentum exchange model. Shading indicates volume fraction of gas. Vectors indicate liquid velocity.**

## Rocky Flats Precipitator

The final simulation to be discussed here is our first attempt at the 3-dimensional simulation of a one-quarter section of the Rocky Flats precipitator. We chose to compute with a one-quarter section to minimize problem size and computational burden while still capturing 3-dimensional effects. The block boundaries of the mesh are seen in Figure 12.

The initial simulation was limited to gas-liquid two-phase flow. The gas was introduced as an internal source of mass and momentum to emulate the method of introduction of gas in the physical unit where gas issues from a quarter inch tube inserted into the column with its opening placed at the bottom of the draft tube. The effect of precipitating solids was ignored.

The simulations were run on a single processor of an HP9000 workstation. It took approximately 23 hours to simulate a real-time second and it took approximately 3 to 4 seconds for the gas plume in the draft tube to reach the top of the column and establish circulation. The results of the initial calculation are shown in Figures 13 and 14. Figure 13 shows the volume contours of gas in the column. It is seen that virtually all of the gas flows up and out of the column and essentially no gas is entrained into the annulus. This behavior is consistent with the Freedman and Davidson bubble column data. Their data indicate that little gas entrainment occurs for low superficial gas feed velocities and for small draft-tube diameters. Liquid circulation is, however, generated as is shown by the velocity vectors in Figure 14.

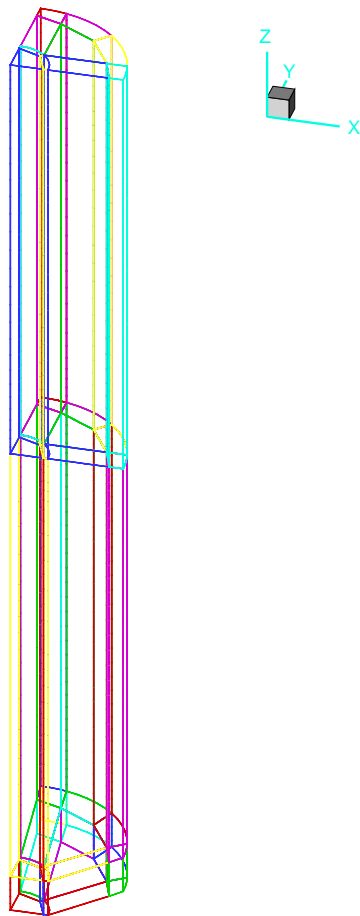


**Figure 12. Block boundaries of the one-quarter section mesh of Rocky Flats draft-tube precipitator.**

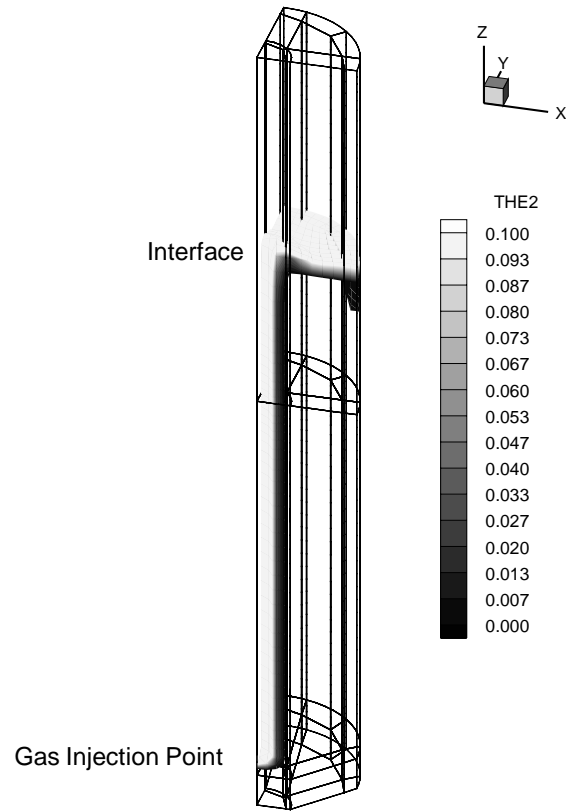


**Figure 13. Gas volume fraction contours in Rocky Flats draft-tube precipitator.**

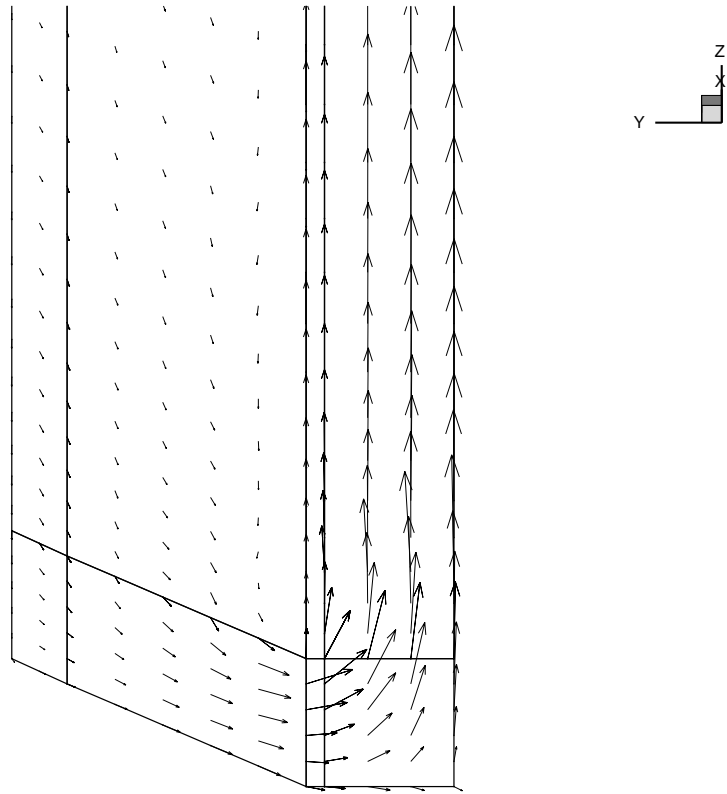


**Figure 14. Liquid velocity vectors at bottom of column.**

## CONCLUSIONS

There are three broad conclusions that can be drawn from the simulation work to date. First, while all the physics associated with turbulent bubble columns is not completely understood, it seems clear that we do have in the CFDLIB computer code the tools with which to attack the problem and obtain some useful results in the not-too-distant future. Second, more work is needed to find the correct or best set of closure models for multiphase turbulence and momentum exchange in these flows. This is a particularly challenging situation when bubble coalescence occurs. Some promising theoretical leads have been recently uncovered in T-3 and should be pursued. Finally, the computational times encountered in the 3-dimensional simulation of the Rocky Flats precipitator suggest the ASCI-class (Accelerated Strategic Computing Initiative class) parallel computing power may need to be used to carry out some of the calculations that will be required.

## REFERENCES

Freedman, W., and J. F. Davidson, "Hold-up and liquid circulation in bubble columns," *Trans. Instn. Chem. Engrs.* **47**, 1969, pp. T251–T262.

Kashiwa, B. A., and R. M. Rauenzahn, "A Multi-Material Formalism," in *Numerical Methods in Multiphase Flows*, FED-Vol. 185, ASME, 1994.

Matysiak, L. M., and M. L. Burns, "Los Alamos Waste Management Cost Estimation Model," Los Alamos National Laboratory report LA-12757-M, March 1994.

Pironti, F. F., V. R. Medina, R. Calvo, and A. E. Saez, "Effect of draft tube position on the hydrodynamics of a draft tube slurry bubble column," *The Chemical Engineering Journal* **60**, 1995, pp. 155–160.

Simonin, O., and P. L. Violette, "Numerical Study on Phase Dispersion Mechanisms in Turbulent Bubbly Flows," International Conference on Mechanics of Two-Phase Flows, June 12–15, 1989, National Taiwan University, Taipei, Taiwan, ROC.

Yarbro, S. L., S. B. Schreiber, S. L. Dunn, and C. W. Mills, "Automated Homogeneous Oxalate Precipitation of Pu(III)," Los Alamos National Laboratory report LA-11936, February 1991.

## APPENDIX

### TECHNICAL TASK PLAN FOR FY 97

**Principal Investigator:** Brian VanderHeyden, T-3, 7-0371    **Program Code:** KB21  
Steve Yarbrow, NMT-2, 7-2333    **Cost Account:** 2000/0000

**Project Start Date:** 1/15/96

**Project End Date:** 9/30/97

#### Budget

	Operating Target (\$K)	Operating Over Target (\$K)	FTEs	Capital (\$K)	GPP (\$K)
FY 97	150	0	0.8	0	0
FY 98	TBD	TBD	TBD	TBD	TBD
FY 99	TBD	TBD	TBD	TBD	TBD

#### Objective

The T-3 multiphase flow code library, CFDLIB, has been used to simulate multiphase flows in 2 and 3 dimensions with complex geometries in a variety of industrial and defense related problems. This project has been using CFDLIB to analyze the flow and process chemistry in the plutonium precipitators with an aim toward providing insight into the effects of vessel geometries and the bubble and particle scale dynamics which govern the efficiencies of the precipitators. Therefore, CFDLIB will simulate proposed modes of operation of the precipitators to provide updated guidelines for operations.

This applied design development project will also include an experimental component in which data would be collected from precipitators to help validate and guide the multiphase exchange and turbulence closure models that will have to be incorporated in CFDLIB to simulate the precipitators. The initial experiments and data will be determined once a preliminary simulation capability is demonstrated. This will help target the experimental work so that it is most useful for developing the closure models. Further experiments can be decided upon based on the results of the simulation project.

#### Background

Successful completion of the DNFSB 94-1 program is a high priority for the Los Alamos National Laboratory. Many of the residues scheduled for recovery are currently liquids, such as analytical returns, or are solids that will be leached or dissolved to remove the plutonium. Therefore, all of the plutonium will have to be precipitated at some point to concentrate the plutonium as an oxide that is suitable for the long-term repackaging program. Therefore, this project supports key laboratory capabilities for processing residues both for 94-1 and eventual pit manufacturing.

Current waste acceptance criteria are being negotiated that will drive the plutonium discard limit to less than or equal to 0.5 microcurie per liter for liquid waste. Optimizing the recovery of plutonium from the precipitation units will help meet or exceed this limit and reduce the cost of downstream waste processing operations. Current precipitation filtrates

are 9400 microcuries per liter. Also, transuranic (TRU) waste costs approximately \$12,000 per 55 gallon drum to process and dispose. Therefore, significant cost savings will be achieved by having higher plutonium recovery efficiencies. Also, the precipitation conditions affect the filtration characteristics of the final product. Better cakes mean faster filtration times and lower overall exposures to the operators.

### **Current Status**

- The module of basic training in CFDLIB I/O and theory is complete.
- The 2-D simulations of the axisymmetric draft-tube bubble column are complete.
- Initial comparisons with available literature data are 85% complete with in-house validation remaining.
- The initial 3-D simulation of the draft-tube bubble column is complete.
- Adjustment of the turbulence closures for the two-phase bubble column to completely account for the entire design and operating parameter space is ongoing.

### **FY 97 Milestones**

1. Adjust exchange models and turbulence models accordingly. This will involve some groundbreaking work since the topic of turbulence and gross phase distribution in bubble columns is a current research topic in the multiphase flow simulation community. August 1, 1997
2. Add particles to represent the precipitating solids. Perform simulations and compare with appropriate data. Determine if exchange or turbulence models require modifications. Some computations may require use of high-speed parallel computing platforms such as the CRAY T3D or a similar ASCI-class machine. This could also take quite a bit of time if the problem proves difficult. July 30, 1997
3. Issue progress report and project evaluation. March 30, 1997
4. Add chemistry to model precipitation reactions and include important rate-limiting processes such as mass transfer resistances. September 30, 1997
5. Begin to generate list of proposed improvements to the precipitators including geometrical changes and operational and procedural changes. Perform CFDLIB simulations and rank proposal based on simulation results. Choose best candidate. September 30, 1997
6. Propose and perform experimental validation of best candidate. January 1998
7. Issue final report and recommendations. June 1998

This report has been reproduced directly from the best available copy.

It is available to DOE and DOE contractors from the Office of Scientific and Technical Information, P.O. Box 62, Oak Ridge, TN 37831. Prices are available from (615) 576-8401.

It is available to the public from the National Technical Information Service, US Department of Commerce, 5285 Port Royal Rd. Springfield, VA 22161.

